Experimental Demonstration of Complex Image Theory and Application to Position Measurement

Darmindra D. Arumugam, *Student Member, IEEE,* Joshua D. Griffin, *Member, IEEE,* and Daniel D. Stancil, *Fellow, IEEE*

***Abstract*—Measurements of the magnetoquasistatic fields generated from a magnetic dipole (an electrically small current loop) located above the earth are presented and compared with calculations using complex image theory. With a horizontal (i.e., the surface normal parallel to the earth) emitting loop located at a height of h and a copolarized horizontal receiving loop located at a height of $z \geq 0$, coupling between the dipoles was measured for distances up to 50 m along a direction perpendicular to the surface normal axes of the loops. Inverting the theoretical expressions to estimate the distance from measured field values resulted in peak and rms distance estimation errors of 23.01 cm and 11.74 cm, respectively, for distances between 1.3 m and 34.2 m. Received signals were not strongly affected by the proximity of a group of people even when the line-of-sight was obstructed.**

***Index Terms*—Electromagnetic fields, magnetoquasistatics, radio tracking, radio position measurement.**

I. Introduction

THE wireless position tracking problem is of increasing relevance to society today owing to applications such as navigation, security, and asset tracking [1], [2]. Despite numerous technological advances, position location systems such as global positioning systems (GPS), ultra-wide band (UWB) systems, and radio frequency identification (RFID) systems suffer reduced performance in non-line-of-sight (NLoS) environments [1] and when in proximity to lossy objects. These drawbacks limit their use for some applications, such as contact sports, in which the line-of-sight (LoS) to the mobile location device may be blocked by player's bodies and the device held close to their body. A promising solution for position tracking in the presence of groups of people is the use of low-frequency, quasistatic magnetic fields instead of propagating radio waves. Quasistatic magnetic fields are largely undisturbed by the human body, can be used to solve for both the position and orientation of the mobile device [3]–[9], and penetrate weakly conducting dielectric materials. They have been used for the localization of medical devices in the body [6], [8] and for below-ground tracking in mines [4]. Further, complex image theory applied to quasistatic magnetic fields has been used to extract underground features from surface measurements [10]. This paper presents a technique to determine the position and orientation of an emitter above a lossy dielectric using quasistatic magnetic fields and complex image theory. The result is improved accuracy for above-ground tracking over distances from approximately 1 m up to several 10s of meters.

Manuscript received December XY, 2010.

D. D. Arumugam is with Disney Research, Pittsburgh, PA, 15213, and the Department of Electrical and Computer Engineering, Carnegie Mellon University, Pittsburgh, PA, 15213 USA e-mail: darumugam@cmu.edu

J. D. Griffin is with Disney Research, Pittsburgh, PA, 15213 USA e-mail: joshdgriffin@disneyresearch.com

D. D. Stancil is with Disney Research, Pittsburgh, PA, 15213, and the Department of Electrical and Computer Engineering, North Carolina State University, Raleigh, NC, 27695 USA e-mail: ddstancil@ncsu.edu

II. Complex Image Theory

After Sommerfeld's 1909 study of an electromagnetic source above a conducting half-space [11], a renewed interest for quasistatic fields was attributed to an observation of a complex image by Ball et al.[1] (see [12], [13]) in 1966 who proposed an image of the source at a complex depth beneath the ground. Following this observation, a number of authors described this quasistatic image theory for specific types of sources [12]–[14]. In 1971, Weaver [13] consolidated these works, describing an arbitrary source in the presence of a conducting half-space. Weaver [13] showed that the fields generated by a source at $z = h$ in the presence of a conducting half-space ($z \leq 0$), shown in Fig. 1, is a function of the fields from the source, its image at a complex depth beneath the ground, and a summation of correction terms (not shown in Fig. 1). The correction terms become negligible further than a skin depth away from the classical mirror image of the source, i.e., when $R^0 >> \delta$, where R^0 is the geometrical distance from the classical image of the source, $\delta = 1/\sqrt{\pi f \mu_0 \sigma}$ is the skin depth, f is the frequency, μ_0 is the permeability of free space, and σ is the ground conductivity. The magnetic fields for this case are [13]

$$H_p(x,y,z) = H_p^s(x,y,z) + c_p H_p^i(x,y,z) + c_p \left[\sum_{n=3}^{\infty} a_n (\frac{\alpha}{2})^n \frac{\partial^n}{\partial \zeta^n} H_p^d(x,y,\zeta) \right]_{\zeta=-z-h-\alpha}, \quad (1)$$

where the summation represents the correction terms, $\alpha = \delta(1-j)$, and a_n are coefficients of a Maclaurin series.[2] The subscript $p = ||, \perp$ indicates the field components parallel and perpendicular to the ground, respectively; the superscripts s and i indicate the fields originating from the source and the complex image, respectively; and $c_{||} = 1$ and $c_{\perp} = -1$. The fields of the source and complex image are $\vec{H}^s(x,y,z) = \vec{H}^d(x,y,z-h)$ and $\vec{H}^i(x,y,z) = \vec{H}^d(x,y,-z-h-\alpha)$,

[1] Wait [12] and Weaver [13] reference an unpublished report by Ball et al. on complex image theory. The authors have not been able to obtain a copy of this report.

[2] From the series expansion of the third term in the exact solutions, we find that $a_n = [1/3, 0, -3/20, 1/18, 5/56, -1/20, \ldots]$ for values of $n \geq 3$.

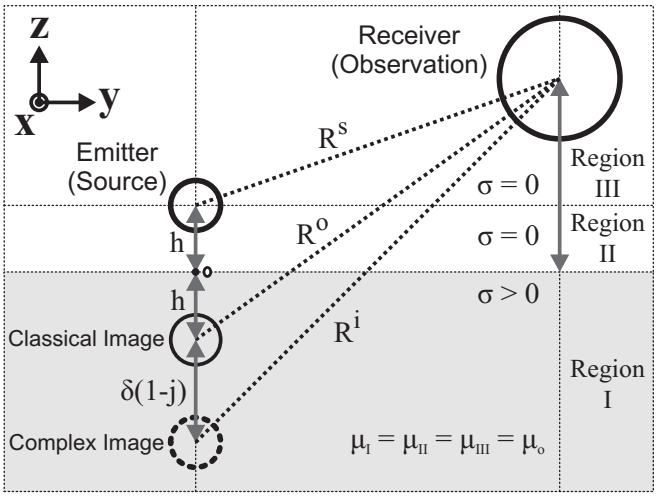

Fig. 1. Complex image theory for magnetoquasistatic fields generated by a source above a conducting half-space.

respectively, where $\vec{H}^d(x,y,z)$ is the field from a magnetic dipole in free space located at the origin. $\vec{H}^d$ is given by

$$\vec{H}^d(x,y,z) = \frac{1}{4\pi}\left[\frac{3\vec{r}(\vec{m}\cdot\vec{r}) - \vec{m}r^2}{r^5}\right], \tag{2}$$

where $\vec{m}$ is the magnetic moment and $\vec{r} = r\hat{r}$ is the position vector from the origin to the point of observation. If the third and higher-order spatial derivatives of $\vec{H}^d$ in (1) are negligible, the complex image theory approximation for the fields is obtained [13]

$$H_p(x,y,z) \approx H_p^s(x,y,z) + c_p H_p^i(x,y,z). \tag{3}$$

Fig. 1 shows a two-dimensional description of complex image theory indicating three regions of observation and a complex image at a depth of $h+\delta(1-j)$ beneath the ground. The circles represent horizontal magnetic dipoles formed by electrically-small current loops aligned with axes along the positive x-axis (HMD$_x$). Equations (1) and (3) are valid in both Region II $(0 < z \leq h)$ and Region III $(z > h)$, but not in Region I $(z \leq 0)$.

III. Application to Position and Orientation Tracking

The theoretical expressions, (1)-(3), relating the position and orientation of the source to the fields at a point of observation assume that the point is within the quasistatic region of the source (i.e., much less than a wavelength). From Faraday's law of induction, the voltage generated at the terminals of a receiving electrically-small, single-loop coil (assuming time-harmonic fields, and a non-permeable space), is expressed as

$$V = -j\omega\mu_o\left[\hat{n}\cdot\left(\vec{H}_{||} + \vec{H}_{\perp}\right)\right]a, \tag{4}$$

where $\hat{n}$ is the unit vector normal to the loop, a is the surface area of the loop, and $\vec{H}_{||}$ and $\vec{H}_{\perp}$ are defined in (3).

If k fixed receivers are used, a system of equations (each representing (4) for the specific receiver) can be expressed in the form [9]

$$V_i^T - V_i^M = 0, \qquad (i = 1, 2, \ldots, k), \tag{5}$$

where V^T represents the induced voltage given by the theoretical expression from (4), and V^M is the measured voltage in the receiving loop. Using the spherical coordinate system, three position (x,y,z) and two orientation (θ,ϕ) unknowns exist, and thus a minimum of five receivers are required to locate a loop. For $k \geq 5$, the optimal solution to (5) can be found using a numerical, non-linear, least-square optimization algorithm to minimize [9]

$$\Phi = \sum_{i=1}^{k}\left[V_i^T - V_i^M\right]^2. \tag{6}$$

If the conductivity σ (and hence the skin depth δ) of the ground is not known, then the conductivity can be obtained by minimizing (6) for $k \geq 6$. The inverse problem of tracking a receiver can be accomplished by using multiple fixed emitters with known position and orientation with the added advantage that, because the emitters are fixed, the depth of the complex image will not change rapidly. For both the case of a mobile emitter or a mobile receiver, the total number of fixed receivers or emitters, respectively, must be greater or equal to the number of unknowns.

IV. Description of Experiment

Position location using complex image theory was demonstrated by moving a small emitting loop relative to a fixed receiving loop. To simplify the problem for this proof-of-concept measurement, the emitter's orientation and height were fixed and it was moved away from the receiving loop in a single direction. This setup corresponds to measuring the H_x field component of the HMD$_x$ configuration described in Fig. 1. The emitting loop consisted of 45 turns of 34 AWG copper wire with a diameter of 16.5 cm. The loop was driven with an rms current of about 225 mA at a frequency of 387 kHz. A signal generator (model E4433B from Agilent Technologies), amplifier (model ZFL-500+ from MiniCircuits), and balun

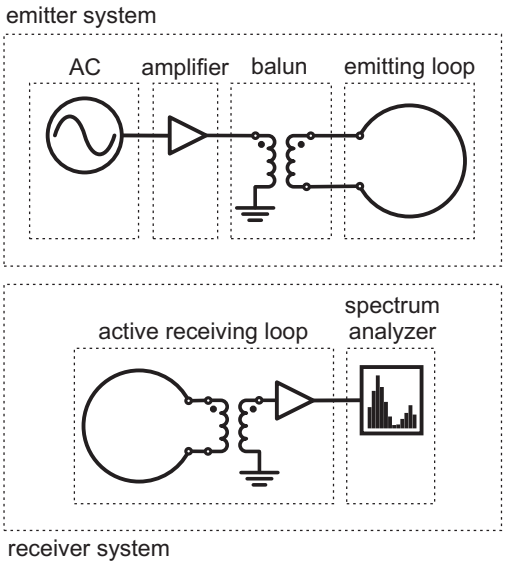

Fig. 2. Block diagram of the experimental measurement system consisting of the emitter and receiver systems.

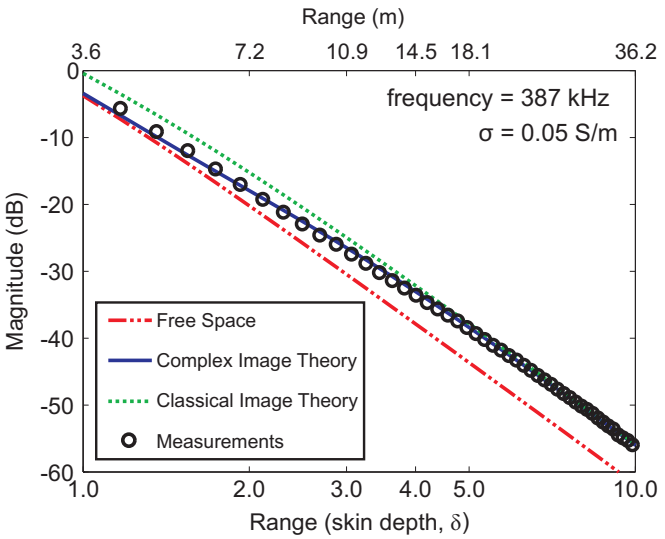

Fig. 3. Theory and measurements for the H_x component of the HMD$_x$ for values of $\delta \leq y \leq 10\delta$ (3.62 m $\leq y \leq$ 36.2 m) over the ground. The magnitude plotted is $|H_x/\,(1\ A/m)|$ in the dB scale.

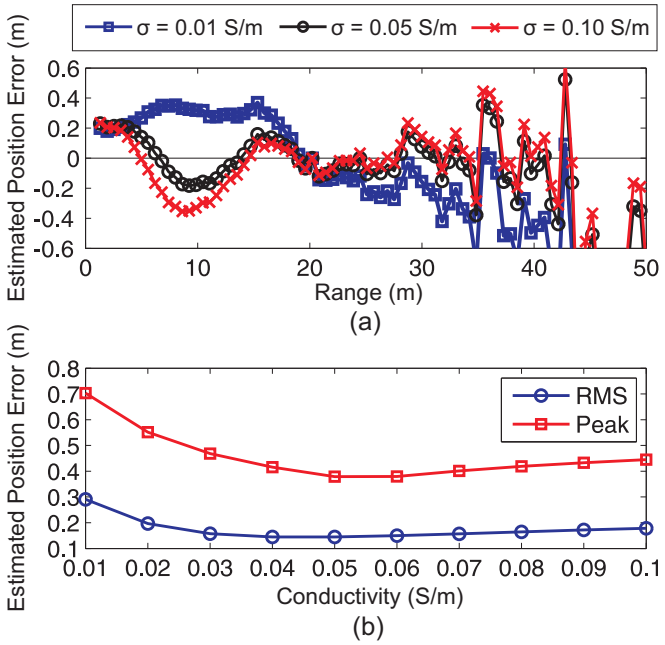

Fig. 4. Position error as a function of distance, obtained using complex image theory.

(model ADT1-6AT-1 from MiniCircuits) were used with the emitting loop. An active receiving loop (model LFL-1010 from Wellbrook Communications) and a spectrum analyzer (model 8593E from Agilent Technologies) were used to measure the fields. The pattern of the emitting loop was measured by rotating it in place while using a single receiving loop. As evidence of proper operation, the measured pattern agreed with that of a magnetic dipole to within 0.76 dB at the broadside of the emitting loop. A block diagram of the measurement system is shown in Fig. 2. For these measurements, the height of the center of the emitting loop was $h = 0.84$ m and the height of the center of the receiving loop was $z = 1.75$ m.

Because the height and orientation of the emitter were fixed, only two unknowns remained in (3): the distance y between the emitter and receiver and the conductivity of earth (which is included in the α term in (1)). Because the single receiving antenna provides adequate information to solve for only one unknown, a ground conductivity of $\sigma = 0.05$ S/m, which is within one order of magnitude of previously measured results [15], was chosen to obtain a good agreement between the theory and measurements. Furthermore, to correct for the unknown system gain, an offset was added to the theory to bring the theory and experiment into agreement at a reference distance of 20.22 m. The measurements are plotted along with theoretical results for complex image theory and classical image theory in Fig. 3. It is clear that complex image theory is in much better agreement with the measurements than the classical theory for a range of less than about 5 skin depths. The estimated position error (difference between estimated and true position) obtained from the measured field strength is shown in Fig. 4a for ground conductivity values of $\sigma =$ 0.01 S/m, $\sigma = 0.05$ S/m, and $\sigma = 0.10$ S/m. The accuracy is better than 24 cm for a range of up to 34.2 m and a ground conductivity of $\sigma = 0.05$ S/m. The RMS and peak error are shown in Fig. 4b for ground conductivity values between 0.01 S/m and 0.1 S/m for distances up to 40.34 m. This accuracy is comparable to or better than that of technologies such as civilian GPS (5-10 m), UWB (0.1-1 m) and RFID (1-2 m) [2], all of which work best with a clear line-of-sight. Differential, real-time kinematic GPS can achieve cm level accuracy, but also requires an unobstructed view of the sky and proper orientation of the antenna. In contrast, because low frequency magnetic fields are not significantly altered by proximity to lossy, non-magnetic dielectrics (e.g., the human body), this technique should offer improved performance in applications where other techniques based on radio wave propagation fail to provide reliable tracking. To verify insensitivity to blocking the line-of-sight, measurements were taken with four people spaced evenly on a circle of diameter $d = 0.76$ m at a distance $a_y = 0.98$ m as illustrated in Fig. 5. The horizontal distance separating the loops was $L = 2.9$ m and the height of the receiver and emitter were, respectively, $z = 1.2$ m and $h = 1.1$ m. The group initially blocked the LoS ($a_x = 0$)

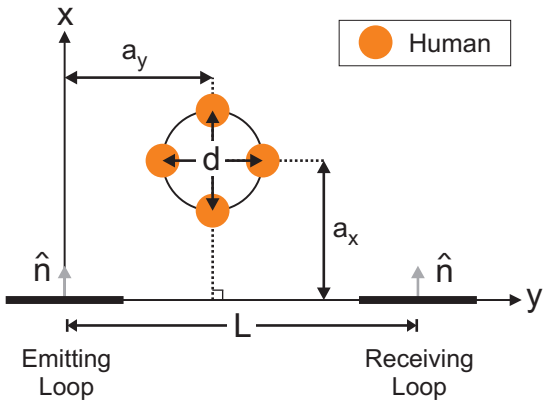

Fig. 5. Measurements with four people spaced evenly on a circle of diameter $d = 0.76$ m at a distance $a_y = 0.98$ m.

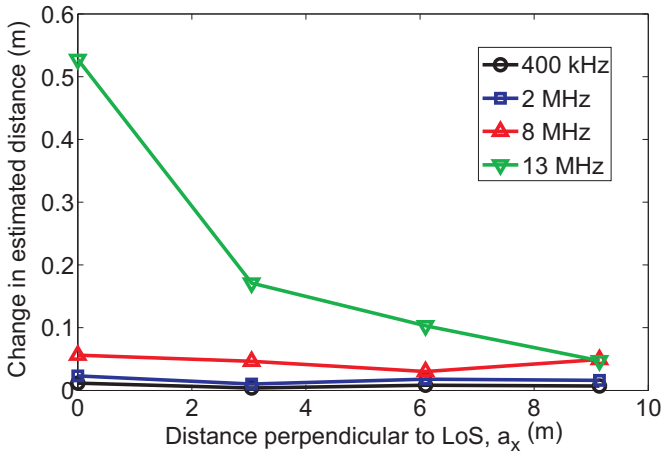

Fig. 6. Change in estimated distance due to the presence of a group of four people at 400 kHz, 2 MHz, 8 MHz, and 13 MHz.

and was moved in the direction perpendicular to the LoS (increasing a_x). The measurement was conducted at multiple frequencies (400 kHz, 2 MHz, 8 MHz, and 13 MHz), and the problem space was within the quasistatic region for all measured frequencies. By measuring the induced voltage in the receiving loop with and without the group of people, the change in estimated distance was computed and is shown in Fig. 6. The use of higher frequencies resulted in an increased change in estimated distance. The peak and average change in estimated distance at 400 kHz due to the presence of the group are 1.16 cm (at $a_x = 0$) and 0.77 cm, respectively, demonstrating that the presence of people has very little effect at the lower frequencies.

V. Conclusions

In summary, we have shown that the use of magnetoquasistatic fields analyzed with complex image theory enables long range (10s of meters) position tracking and operates when in proximity to groups of people – even when the line-of-sight is blocked.

Acknowledgment

The authors would like to thank David S. Ricketts for useful discussions.

References

[1] K. Krizman, T. Biedka, and T. Rappaport, "Wireless Position Location: Fundamentals, Implementation Strategies, and Sources of Error," in *IEEE Vehicular Tech.*, vol. 47, no. 2, 1997, pp. 919–923.

[2] H. Liu, H. Darabi, P. Banerjee, and J. Liu, "Survey of Wireless Indoor Positioning Techniques and Systems," in *IEEE Trans. Sys., Man, and Cybernetics*, vol. 37, no. 6, November 2007, pp. 1067–1080.

[3] F. Raab, "Quasi-static magnetic-field technique for determining position and orientation," *IEEE Trans. on Geoscience and Remote Sensing*, vol. GE-19, no. 4, pp. 235–243, October 1981.

[4] L. H. Rorden and T. C. Moore, "Method and apparatus employing received independent magnetic field components of a transmitted alternating magnetic field for determining location," US Patent No. 4,710,708, December 1 1987.

[5] J. S. Bladen and A. P. Anderson, "Position location system," US Patent No. 5,913,820, June 22 1999.

[6] M. Schneider, "Measuring position and orientation using magnetic fields," US Patent No. 6,073,043, June 6 2000.

[7] N. Amorai-Moriya, M. Itzkovich, and B. Spivak, "System for three dimensional positioning and tracking," US Patent No. 6,316,934, November 13 2001.

[8] A. Govari, "Electromagnetic position single axis system," US Patent No. 6,484,118, Nov. 19 2002.

[9] A. Plotkin and E. Paperno, "3-D Magnetic Tracking of a Single Subminiature Coil with a Large 2-D Array of Uniaxial Transmitters," in *IEEE Trans. Magnetics*, vol. 39, no. 5, Sept. 2003, pp. 3295–3297.

[10] W. Anderson, "Approximate inversion of high-frequency electromagnetic soundings using complex image theory," *Geophysics*, vol. 56, no. 7, pp. 1087–1092, July 1991.

[11] A. Sommerfeld, "Uber die Ausbreitung der Wellen in der drahtlosen Telegraphie," in *Ann. Phys. Leipz.*, vol. 28, no. 4, 1909, pp. 665–736.

[12] J. Wait, "Image theory of a quasistatic magnetic dipole over a dissipative half-space," in *Electronics Letters*, vol. 5, no. 13, June 1969, pp. 281–282.

[13] J. Weaver, "Image approximation for an arbitrary quasi-static field in the presence of a conducting half space," in *Radio Science*, vol. 6, no. 6, June 1971, pp. 647–653.

[14] P. Bannister, "Summary of image theory expressions for the quasi-static fields of antennas at or above the earth's surface," in *Proceedings of the IEEE*, vol. 67, no. 7, July 1979, pp. 1001–1008.

[15] H. Fine, "An Effective Ground Conductivity Map for Continental United States," in *Proceedings of the IRE*, vol. 42, no. 9, September 1954, pp. 1405–1408.